Accurate Passive Component Models in Coplanar Waveguide for 50 GHz MMICs

R. Shimon, D. Scherrer, D. Caruth, J. Middleton, H. Hsia, and M. Feng

Department of Electrical and Computer Engineering
Center for Compound Semiconductor Microelectronics
University of Illinois at Urbana-Champaign
Urbana, Illinois 61801

Abstract—Accurate circuit models for several passive components in coplanar waveguide have been developed. These models utilize lumped and distributed circuit elements available in computer-aided design software packages and have element values that are derived from measured *S*-parameter data, geometrical data and physical process parameters. This work discusses the development of the models and verifies their accuracy by comparing measured and modeled *S*-parameters to 50 GHz.

I. INTRODUCTION

Circuit models for passive components are necessary to accurately predict the performance of matching and filtering networks in MMIC designs. Most often planar electromagnetic simulators are employed to predict the performance of passive structures not available in computer-aided design (CAD) software element libraries. This method has been used with much success, but the process is time-consuming and the data generated cannot be optimized along with the rest of the circuit.

The models developed here differ in that they consist entirely of lumped or distributed elements available in CAD packages and are derived from measured *S*-parameter data, geometrical data and physical process parameters. These models provide accurate and easily implemented representations of the passive structures and have been used at the University of Illinois to successfully develop MMIC amplifiers and oscillators at 24 and 38 GHz in both MESFET and HBT technologies [1,2].

All of the models described below were implemented in Hewlett Packard's Microwave Design System (MDS). For each passive component, the proposed model is presented along with plots displaying the measured and simulated values of *s11* and *s21*. Markers on many of the plots indicate the values of the *S*-parameters at 38 GHz.

When appropriate, two quantitative measures of error are given: the difference in the magnitudes of the measured and simulated data, expressed as a percent and averaged over frequency, and the difference in the phases of the measured and simulated data, also averaged over frequency. Standard deviations of these errors are also given as estimates of worst case error.

II. FABRICATION AND MEASUREMENT

All of the CPW structures examined in this work were fabricated at the University of Illinois on a semi-insulating GaAs substrate using a standard, three metal process. The CPW transmission line and capacitor bottom are patterned on Metal1, the capacitor top is patterned on Metal2, and the ground tie is formed from ABMetal. Table I lists the process layers and the electrical and geometrical parameters for each layer.

TABLE I
UIUC Process Layers and Parameters

Process Layer	Process Parameters
ABMetal	t = 3 µm
ABVia	h = 3 µm
Metal2	t = 0.6 µm
CapDie	εeff = 6.55
	h = 0.2 µm
Metal1	t = 1 µm
SI GaAs	εeff = 13.1
	h = 635 µm

S-parameter measurements were made using a Hewlett Packard 8510C Network Analyzer with GGB coplanar ground-signal-ground probes. On-wafer short, open, load and thru standards were used to calibrate the analyzer. These standards have identical pad and taper dimensions as those used to probe the structures under test. They are designed so that the measurement planes are positioned after the probe-to-CPW transitions, thus removing them from the measured *S*-parameters.

III. PASSIVE COMPONENT MODELS

A. CPW Transmission Line

MDS's CPW transmission line model was used to simulate an array of 750 µm long lines of varying center conductor widths and gaps. The values of ER, COND and TAND in the substrate definition were optimized so that the model best fit the measurement of our standard 50 Ω transmission line. This line has a 20 µm wide center conductor and a 15 µm gap. Table II lists these values. The magnitude error in *s21* is -0.2% with a sigma of 2.0%, and the phase error in *s21* is -0.05° with a sigma of 0.8°.

0-7803-4603-6/97/$5.00 (c) IEEE

TABLE II
UIUC CPW Substrate Definition

Element	Value
εr	ER=14.1
μr	MUR=1
σ	COND=2.73e+7
$tan\delta$	TAND=0.01

The characteristic impedance, effective permittivity and loss per unit length were extracted from the measured and simulated data for each combination of width and gap. Figure 1 shows these values for the various dimensions at a frequency of 38 GHz. The values obtained here are in general agreement with previously published results [3]. The model accurately predicts the line's characteristic impedance and fairly accurately predicts the line's loss per unit length for all values of width and gap.

The model does not, however, accurately predict the line's effective permittivity for small values of width or gap. The presence of the capacitor dielectric above the line causes the effective permittivity for these thin, high impedance lines to be larger than that predicted by the model. As an example, the model underestimates the electrical length of a quarter-wavelength long line with a 5 μm width and 5 μm gap by 5.8°.

B. CPW Bend

An analysis of CPW meander lines indicates that the effect of the CPW bend is seen as a slight reduction in the centerline length of the line. A length correction factor for bend angles of 45° and 90° was calculated from measurements of 400 μm long meander lines. These factors were then verified by comparing the measured and simulated *s*-parameters of 1600 μm long meander lines. To investigate the effects of the ground tie on the transmission characteristics of the line, one set of structures was fabricated with ground ties between each bend; another set was fabricated without any ground ties. Figure 2 shows the CAD drawing for two such structures.

Typical plots of *s11* and *s21* are shown in Figure 3. The measured reflection coefficients for all of the structures were below -25 dB across the entire band, indicating that reflections from the bend discontinuities are small. The structures without ground ties exhibited slightly lower reflection coefficients. The calculated length correction factor for a 90° bend angle without ground ties is -13.3 μm/bend; the correction factor for a 45° bend angle without ground ties is -4.2 μm/bend. With these corrections, the magnitude error in *s21*, for both bend angles, is -1.7% with a sigma of 1.5%. The phase error in *s21*, for both bend angles, is -0.1° with a sigma of 0.6°.

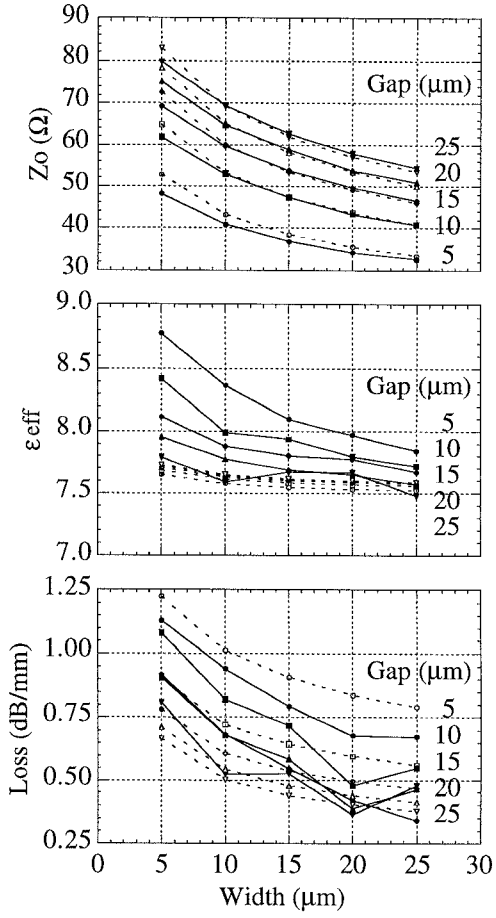

Fig. 1. The characteristic impedance, effective permittivity and loss per unit length of a CPW line for various line widths and gaps at 38 GHz. The solid lines represent measured data; the dashed lines represent simulated data.

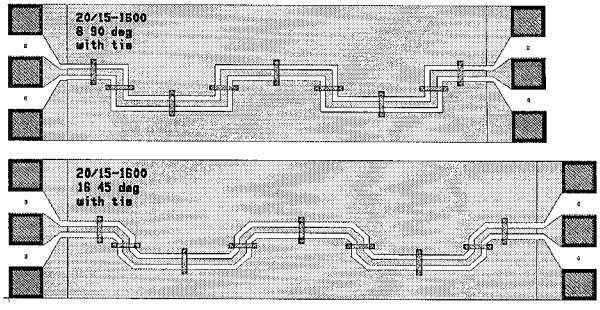

Fig. 2. Two 50 Ω CPW meander lines. The top structure contains eight 90° bends; the bottom one contains 16 45° bends.

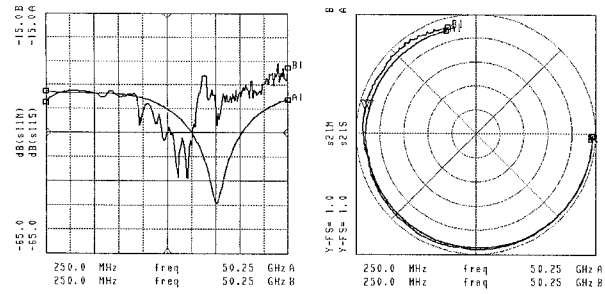

Fig. 3. Measured (M) and simulated (S) *s11* and *s21* for a 50 Ω CPW meander line with 16 45° bends.

C. CPW T-junction

An analysis of the CPW T-junction reveals that the lumped element equivalent circuit shown in Figure 4 fairly accurately characterizes the field storage effects present at the discontinuity [4]. The measured *S*-parameters of three tee structures, each with a different impedance terminating the third port, were used to optimize the values of the lumped inductances and capacitance of the model. Figure 4 shows a CAD drawing for one of these tee structures.

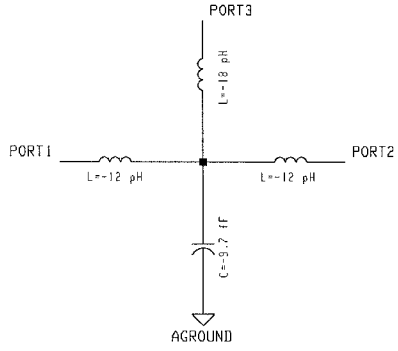

Fig. 4. Equivalent circuit for the symmetric, 50 Ω CPW T-junction.

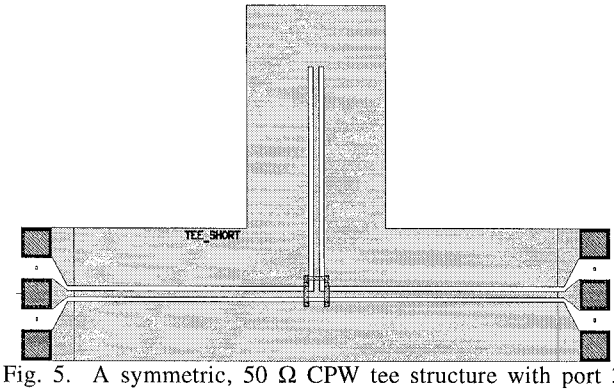

Fig. 5. A symmetric, 50 Ω CPW tee structure with port 3 terminated in a short circuit.

The value of the inductors in series with ports 1 and 2 is -12 pH, while the value of the inductor in series with port 3 is -18 pH. The value of the shunt capacitance is -9.7 fF. The position of the three T-junction reference planes is consistent with the convention used in microstrip T-junction models. That is, the lengths of the transmission lines at ports 1 and 2 are measured from the probe pads to the centerline of the stub at port 3. The length of the stub is measured from the edge of these lines to the termination.

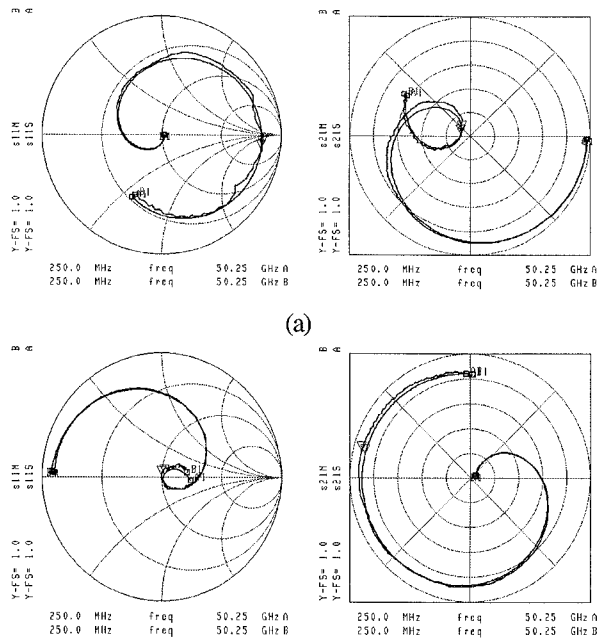

(a)

(b)

Fig. 6. Calculated (M) and simulated (S) *s11* and *s21* for the symmetric, 50 Ω CPW T-junction with port 3 terminated in (a) an open circuit and (b) a short circuit.

Figure 6 shows typical plots of *s11* and *s21* for T-junctions with port 3 terminated in an open and short circuit. It is difficult to quote meaningful magnitude or phase errors for either structure, since the magnitudes of both *s11* and *s21* vary widely with frequency. However, the model does predict both the minimum in $|s21|$ of Figure 6(a) and the minimum in $|s11|$ of Figure 6(b) with considerable accuracy. Errors in phase, where they can be meaningfully defined, are generally less than 3°.

D. CPW Capacitor

The MIM capacitor is a three conductor system characterized by even and odd mode impedances and phase velocities. The odd mode, contained between the plates of the capacitor, is the desired and dominant mode. At frequencies where the electrical length of the capacitor is significant, however, the effects of the even mode, the coplanar mode, may be dramatic. If the even mode impedance is less than 50 Ω, the even mode appears as a shunt capacitance. If the even mode impedance is greater than 50 Ω, the even mode appears as a series inductance.

Values for the even and odd mode parameters may be estimated as follows. The even mode impedance is approximately twice the characteristic impedance of a CPW line of identical dimensions. The even mode effective permittivity is approximately equal to the effective permittivity of the identical CPW line, and the odd mode effective permittivity is approximately equal to the relative permittivity of the capacitor dielectric. The resulting odd mode impedance may then be calculated from these numbers using coupled line theory. Figure 7 shows the model. Large valued resistors in the model simulate open circuits.

Three 500 μm long capacitors, all with a 20 μm center conductor width and varying gaps, were measured. Figure 8 shows typical plots of *s11* and *s21* for capacitors with 5 μm and 25 μm gaps. The effects of the even mode appear for both geometries: a capacitive tail is evident in the former, while an inductive tail is evident in the latter. These same effects are absent in the measurements of a capacitor with a 15 μm gap. This is an expected result, as these dimensions correspond to a characteristic impedance close to 50 Ω.

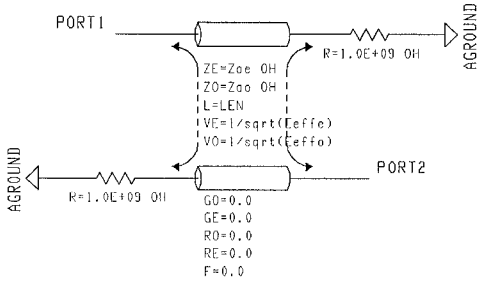

Fig. 7. Coupled transmission line model for the CPW capacitor.

The magnitude error in *s21* for the 5 μm gap capacitor is 5.1% with a sigma of 2.8%; the phase error is 3.2° with a sigma of 1.8°. The 25 μm gap capacitor model was more accurate. The magnitude error in s21 is 1.5% with a sigma of 1.1%; the phase error is 1.0° with a sigma of 1.1°.

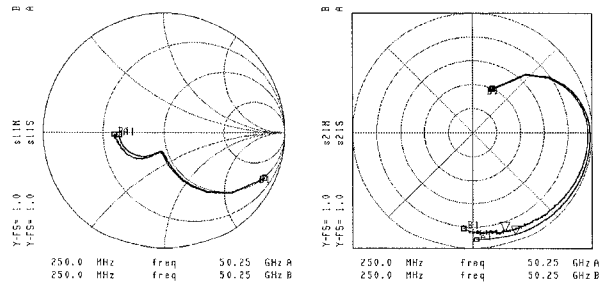

(a)

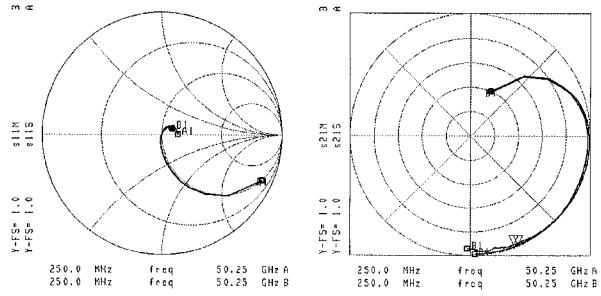

(b)

Fig. 8. Measured (M) and simulated (S) *s11* and *s21* for CPW capacitors with a 20 μm center conductor width and (a) a 5 μm gap and (b) a 25 μm gap.

IV. CONCLUSION

This work presents models for several passive CPW structures and verifies their accuracy to 50 GHz by comparing the measured and simulated *S*-parameters. The models consist of lumped and distributed elements with values that are derived from the measured *S*-parameters, geometrical data and physical process parameters. Each is easily implemented in commercial circuit simulators, yet provides sufficient accuracy for many MMIC designs.

REFERENCES

[1] J. R. Middleton, D. S. Chen, C. C. Teng, J. Kruse, D. Scherrer, R. Shimon, D. Barlage, M. Heins and M. Feng, "Design and Fabrication of Coplanar Ka-Band Monolithic Integrated Circuits," in *1996 U.S. Conference on GaAs Manufacturing Technology.*

[2] M. S. Heins, D. W. Barlage, M. T. Fresina, D. A. Ahmari, Q. J. Hartmann, G. E. Stillman and M. Feng, "Low Phase Noise Ka-Band VCOs using InGaP/GaAs HBTs and Coplanar Waveguide," to be published in *1997 IEEE MTT-S Int. Microwave Symp. Dig.*

[3] W. H. Haydl, J. Braunstein, T. Kitazawa, M. Schlechtweg, P. Taskar and L. F. Eastman, "Attenuation of Millimeterwave Coplanar Lines on Gallium Arsenide and Indium Phosphide Over the Range 1-60 GHz," in *1992 IEEE MTT-S Int. Microwave Symp. Dig.*, pp. 349-352.

[4] K. C. Gupta, Ramesh Garg and I. J. Bahl, *Microstrip Lines and Slotlines.* Artech House, Dedham, Massachusetts: 1979.